Journal of Applied Mechanics and Technical Physics, Vol. 49, No. 1, pp. 53–57, 2008

DISCHARGE AND ENERGY-LOSS COEFFICIENTS IN FLOW THROUGH A BREACH IN A TRAPEZOIDAL DAM

V. I. Bukreev,[1] **V. V. Degtyarev,**[2] **and A. V. Chebotnikov**[2]

UDC 532.532.+532.59

The paper presents experimental data on the discharge and energy-loss coefficients for two weirs of polygonal profiles with lateral contraction, which are required, in particular, in simulations of partial dam-break waves. It is shown that the values of these coefficients for a trapezoidal weir with a slope ratio of $1:3$ *differ insignificantly from their values for a rectangular weir.*

Key words: *dam-break waves, breach, discharge and energy-loss coefficients.*

Partial dam break results in the formation of a breach is formed whose cross-sectional area is smaller than the cross-sectional area of the channel at the dam site. Khristianovich [1] proposed a method for solving the corresponding model problem using the first shallow-water approximation, in which the discharge is specified from experiment, unlike in the method of solving the classical total-break problem [1, 2]. Because of the three-dimensional nature of the flow in the vicinity of the breach, it still remains necessary to use additional empirical information in calculations of partial dam-break waves. The theory of [1] assumes that after dam break, the flow in the vicinity of the breach rapidly becomes steady-state. Experiments [3, 4] have supported this assumption. Therefore, in calculations using the method proposed in [1], it is sufficient to know the discharge coefficient for steady-state flow through a weir in the form of a breach. The shape and dimensions of the breach have a significant effect on the discharge.

Available experimental data on the discharge coefficients of weirs of various shapes are given in hydraulic handbooks [5]. The present papers seeks to supplement this information. Because experimental data on weir flow characteristics are needed not only in calculations of partial break-dam problems using the method proposed in [1], the energy-loss coefficient was also measured in the experiments, along with the discharge coefficient.

The real conditions of a partial dam break are modeled by a weir with a polygonal profile and lateral contraction [5]. A diagram of such a weir is presented in Fig. 1. The present reports results of experiments with weirs of rectangular cross section (slope of the upper and lower sides $\beta = \pi/2$) and of trapezoidal cross section ($\tan\beta = 1/3$) (see Fig. 1). Only the discharge and energy-loss coefficients are considered. Some information on the free-surface level established ahead of a rectangular breach after a partial dam break is given in [3, 4]. Experimental data on the discharge coefficient of a rectangular weir is contained in [5]. These data are used in the present work to test the research technique and are supplemented by data on the energy-loss coefficient. In the case of a trapezoidal weir, the entire information obtained is of interest.

The experiments were performed in a rectangular channel of width $B = 20$ cm, height 25 cm, and length 7 m with an even horizontal bottom. Although the channel has relatively small cross-sectional dimensions, it provides Reynolds number such the flow characteristics do not depend on this parameter. The influence of the Reynolds number is discussed in greater detail below.

[1]Lavrent'ev Institute of Hydrodynamics, Siberian Division, Russian Academy of Sciences, Novosibirsk 630090; bukreev@hydro.nsc.ru. [2]Novosibirsk State University of Architecture and Building, Novosibirsk 630008. Translated from Prikladnaya Mekhanika i Tekhnicheskaya Fizika, Vol. 49, No. 1, pp. 68–73, January–February, 2008. Original article submitted September 22, 2006; revision submitted August 20, 2007.

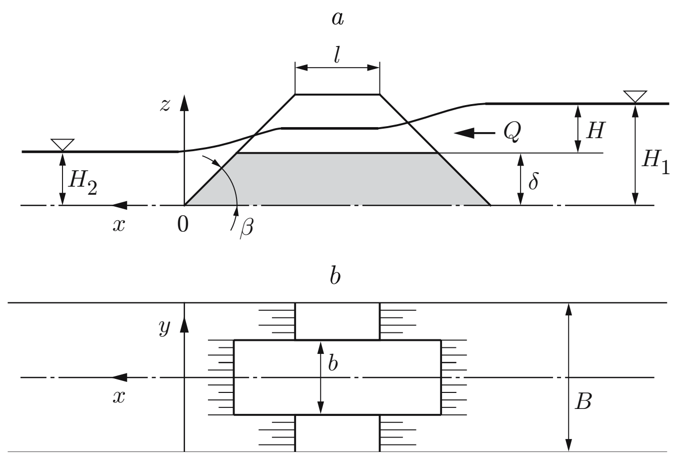

Fig. 1. Flow diagram: (a) longitudinal section; (b) top view.

In all experiments, the breach width was $b = 6$ cm ($b/B = 0.3$), the weir crest height $\delta = 7.2$ cm, and the parameter $l = 38$ cm (see Fig. 1). In addition to the side slope β, the varied parameters in the experiments were the discharge Q, the head above the weir crest H, and the initial tailwater depth H_{20}. Discharge was measured with a standard Venturi flow meter, which was preliminarily calibrated by a volumetric method. Free-surface levels were determined from readings of piezometers located at points at which the pressure distribution with depth was invariably hydrostatic. In some control experiments, piezometer readings were checked by measuring needles.

The discharge coefficient m is determined by the formula [5]

$$m = Q/(bH\sqrt{2gH}\,),$$

where g is the acceleration due to gravity. In the cross sections of steady-state free surface flow with a hydrostatic pressure distribution, the specific energy of the cross section e, which has the dimension of length, is determined by the formula [5]

$$e = h + \alpha_e u^2/(2g).$$

Here h is the flow depth, α_e is the kinetic energy correction [5], $u = Q/S$ is the averaged fluid velocity, and S is the flow cross-sectional area considered. By the definition [5], the water flow depth is the distance from the free surface to the channel bottom. Below, the parameters e, h, β, and u with subscript 1 correspond to the headwater region and those with subscript 2 to the tailwater region. The energy-loss coefficient ζ is defined by the formula [5]

$$\zeta = (e_1 - e_2)/e_1. \tag{1}$$

For the calculations using this formula, we will use the value $\alpha_e = 1$. This imposes additional constraints on the choice of the cross sections in which only the parameters e_1 and e_2 are determined. In these cross sections, not only should the vertical pressure distribution be hydrostatic but also the values of α_1 and α_2 should differ little from unity, which is typical of developed turbulent flow in a channel. The small difference from the value used in the calculations $\alpha_e = 1$ is taken into account by the empirical coefficient ζ. In the experiments, the piezometers were placed so that, in the case of their displacement for a distance $\pm 10H$ along the x axis, the changes in the values of m and ζ did not exceed the measurement error. This error can be judged from the scatter of the experimental points in Figs. 2–5.

Considering the real dam-break conditions, the experiments were performed as follows. We specified several values of the initial tailwater depth H_{20}, for each of which the steady-state discharge value was varied from 0.25 to 4 liters/sec. Measurements were made when the parameters H_1 and H_2 reached constant values. The value of H_2 could differ from H_{20} (in the present experiments, $H_2 < H_{20}$).

As is known, in a certain range of parameters of the problem, a critical depth is established in some cross section above the weirs [3–5], which is calculated by the formula

$$h_* = (q^2/g)^{1/3}, \qquad q = Q/B.$$

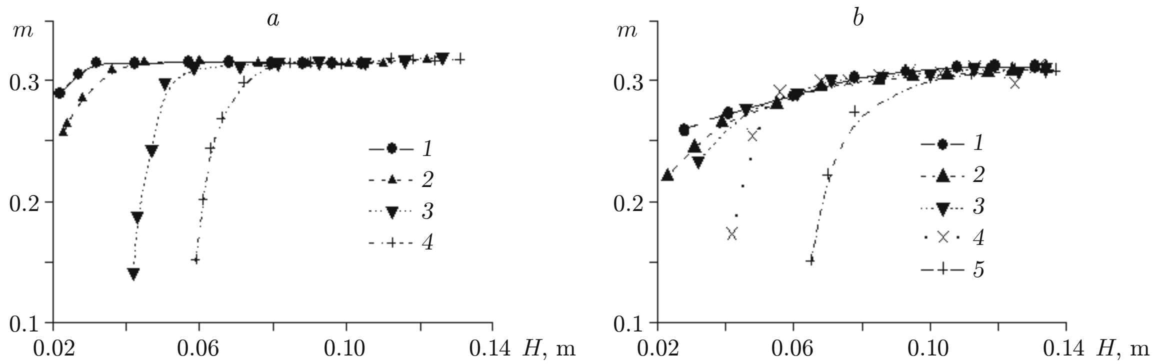

Fig. 2. Discharge coefficient versus head above the weir crest: (a) rectangular weir [$H_{20} = 7.2$ (1), 9.4 (2), 11.35 (3), and 12.9 cm (4)]; (b) trapezoidal weir [$H_{20} = 7.2$ (1), 8.3 (2), 9.4 (3), 11.2 cm (4), and 13.4 cm (5)].

If $H_2 < h_* + \delta$, the state of head and tail conjugation is invariably free. The influence of the submergence of the weir crest is characterized by the dimensionless parameter

$$P^0 = (H_2 - \delta)/h_*.$$

Only positive values of P^0 have a physical meaning.

According to the method used in hydraulics to represent the functions considered [5], the argument in Figs. 2, 4, and 5 is the dimensional head above the weir crest H; therefore, the dependences shown in these figures can be used only for water. To use them for any incompressible Newtonian fluid, it is necessary to transform to the argument $H^0 = Hg^{1/3}/\nu^{2/3}$, where ν is the kinematic viscosity of the fluid considered. This transformation leads only to a scale change on the abscissa. To perform the transformation, it is necessary to multiply H by $g^{1/3}/\nu_w^{2/3}$, where ν_w is the kinematic viscosity coefficient of water at a temperature of 16 °C which corresponds to the conditions of the experiments considered.

Figure 2 shows dependences of m on H for various values of H_{20} for rectangular and trapezoidal weirs. For a rectangular weir and the nonsubmerged weir crest, the coefficient $m \approx 0.314$ for all values of H_{20} and H exceeding a certain value H_*, which is in good agreement with the data shown in [5]. In the free state for $H < H_*$, the influence of the Reynolds number takes place and the coefficient m decreases. From Fig. 2a it follows that, in the case $H_{20}/\delta = 1$, where the state of conjugation is free for all values of H, we have $H_* = 4$–5 cm. The deviation of the discharge coefficient from its asymptotic values for the other values of $H_{20}^0 = H_{20}/\delta$ in Fig. 2a is due to the submergence of the weir crest.

In the free state, it is expedient to determine the threshold value of the Reynolds number Re_* above which the viscosity effect can be ignored:

$$\mathrm{Re}_* = V_* h_*/\nu = mH_*\sqrt{2gH_*}/\nu.$$

In the experiments considered, $\mathrm{Re}_* = 1.55 \cdot 10^4$ (for $H = H_* = 5$ cm). For $\mathrm{Re}_* > 1.55 \cdot 10^4$, the difference between the discharge coefficient and its asymptotic value $m = 0.314$ does not exceed 3%.

For the trapezoidal weir (Fig. 2b), the most important feature of the discharge coefficient is that, even in the region of universality for the parameters H_{20}/δ, P^0, and the Reynolds number, there is a range in which the value of m depends on the head above the weir crest H. The conditions on the sloping lateral sides of such a weir differ from the conditions on the vertical sides of the rectangular weir. In particular, part of the fluid flowing through the sloping side has a vertical velocity component and makes no contribution to the longitudinal component of the angular momentum.

Figure 3 shows the dependence of the discharge coefficient versus the degree of submergence P^0 for a rectangular weir. For physical reasons, the influence of this parameter can manifest itself only in the case $P^0 > 1$, where the difference between the tailwater depth and the height of the weir crest exceeds the critical depth. In the case $b/B = 1$, the influence of submergence shows up only in the range $P^0 > 1.2$–1.3 [5]. The data in Fig. 3 confirm this conclusion for the value of b/B considered in the present paper.

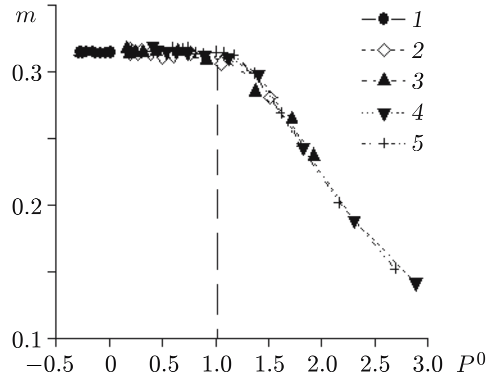

Fig. 3. Discharge coefficient versus the degree of submergence for a rectangular weir: $H_{20} = 7.2$ (1), 8.95 (2), 9.4 (3), 11.35 (4), and 12.9 cm (5).

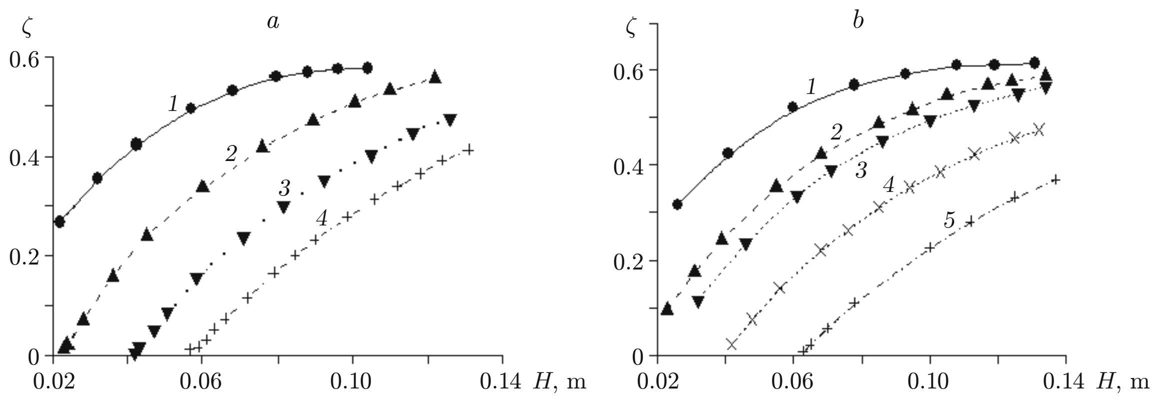

Fig. 4. Energy-loss coefficient versus head above the weir crest: (a) rectangular weir: [$H_{20} = 7.2$ (1), 9.4 (2), 11.35 (3), and 12.9 (4)]; (b) trapezoidal weir [$H_{20} = 7.2$ (1), 8.3 (2), 9.4 (3), 11.2 (4), and 13.4 cm (5)].

Figure 4 shows the energy-loss coefficient ζ determined from formula (1) versus the weir crest head H. Figure 4a corresponds to a rectangular weir, and Fig. 4b to a trapezoidal weir. From Fig. 4 it follows that the energy-loss coefficient depends significantly on the initial tailwater depth. The smaller this depth, other things being equal, the greater the energy loss. These losses are rather significant. For $H_{20} = 7.2$ cm (free state) and $H = 10$ cm, only 45% of the energy of the headwater region remains in the tailwater at a distance $x/H_2 = 100$ from the dam. The energy loss decreases with increasing degree of submergence.

Figure 5 gives experimental data on the energy-loss coefficient ζ_0 at the entrance to rectangular and trapezoidal weirs. The coefficient ζ_0 was determined by the formulas

$$\zeta_0 = \frac{e_1 - e_0}{e_1}, \qquad e_0 = h_* + \frac{V_*}{2g}, \qquad V_* = \frac{Q}{bh_*}. \tag{2}$$

For the submerged state, formulas (2) are inapplicable; therefore, the experimental points in Fig. 5 are given only for the free state. A comparison with the corresponding data in Fig. 4 shows that the energy loss at the entrance makes a significant contribution to the total loss.

Generally, the experiments show that, in calculations of waves generated by a partial break of a trapezoidal dam with a slope ratio of the upper and lower sides of 1 : 3, one can without great error use the values of the discharge and energy-loss coefficients for a rectangular weir with the same values of the parameters b, δ, and l, especially at high heads above the weir crest. If for the parameter l/H of the rectangular weir, the condition $2 < l/H < 12$–15 is satisfied, one can also use available reference data for a broad-crested weir [5].

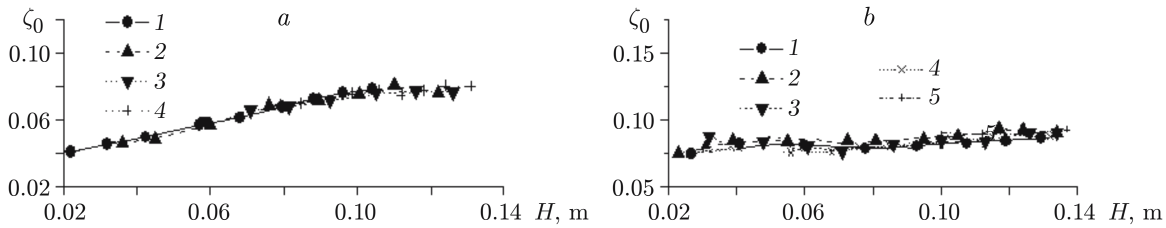

Fig. 5. Energy-loss coefficient at the entrance to the breach versus head above the weir crest (notation the same as in Fig. 4).

We note that in calculations of the discharge and the energy delivered to the tailwater region after dam break, H is taken to be not the initial head above the breach crest $h_- - \delta$, but the smaller parameter H_p determined by transfer of part of the energy to the headwater region. In the case of total dam break and the free state of conjugation, only 2/3 of the initial energy of the headwater region is transferred above the channel bottom to the tailwater region, and 1/3 is transferred upstream by the level depression wave [1, 2]. Preliminary experiments with removal of the shield producing the initial free-surface level difference ahead of a rectangular weir showed that, for the free state, $H_p/H = 0.9$.

This work was supported by the Russian Foundation for Basic Research (Grant No. 07-01-00015) and Program of the Division of the Russian Academy of Sciences (No. 4.14.1).

REFERENCES

1. S. A. Khristianovich, "Unsteady motion in channels and rivers," in: *Some New Problem of Continuum Mechanics* [in Russian], Izd. Akad. Nauk SSSR, Moscow–Leningrad (1938), pp. 15–154.
2. J. J. Stoker, *Water Waves. Mathematical Theory and Applications*, Interscience Publishers, New York (1959).
3. V. I. Bukreev, "On the water depth in the breach during a partial dam break," *Fluid Dynamics*, **40**, No. 5, 769–776 (2005).
4. V. I. Bukreev, "On the discharge characteristic at the dam site after dam break," *J. Appl. Mech. Tech. Phys.*, **47**, No. 5, 679–687 (2006).
5. P. G. Kiselev (ed.), *Handbook on Hydraulic Calculations* [in Russian], Énergiya, Moscow (1972).